Seonghyeon Kim, M. Ercan Altinsoy

Comprehensive Active Control of Booming Noise Inside a Vehicle Caused by the Engine and the Driveline

SLUB
Wir führen Wissen.

TECHNISCHE UNIVERSITÄT DRESDEN

Qucosa
Quality Content of Saxony

Comprehensive Active Control of Booming Noise Inside a Vehicle Caused by the Engine and the Driveline

SEONGHYEON KIM AND M. ERCAN ALTINSOY

Chair of Acoustics and Haptics, Institute of Acoustics and Speech Communication, Technische Universität Dresden, 01069 Dresden, Germany

Corresponding author: Seonghyeon Kim (seonghyeon.kim@tu-dresden.de)

ABSTRACT This study presents comprehensive active cancellation of booming noise caused by the engine and the driveline inside a passenger car. In modern noise control systems for vehicles, booming noise caused by engine harmonics could be effectively suppressed by employing active noise control. However, practical attempts or studies for the active suppression of driveline booming noise are scarce. One of the reasons may be that since the booming noise caused by the driveline is not harmonic with the engine speed, reference signals cannot be generated conventionally. Thus, passive approaches are generally employed to improve the driveline noise. To address this limitation, we propose a method for generating reference signals from engine revolution speed to suppress the driveline noise, such as propeller shaft and tire noise. Reference signals for driveline noise suppression were generated using the information from the torque converter, gear ratio, and final drive ratio. A practical active noise control system was implemented in a six-cylindered large sedan to validate the proposed method. The experimental results showed that the engine firing order was suppressed by 8.0 dB. Moreover, the first order of the propeller shaft and the second and third orders of the tires were suppressed by 5.5 dB, 3.9 dB, and 2.3 dB for entire seat positions. Furthermore, the results presented in this study were considered effective for improving annoyance perception through subjective evaluation.

INDEX TERMS Active noise control, adaptive notch filter, annoyance, booming noise, engine noise, driveline noise.

I. INTRODUCTION

Over the past three decades, active noise control (ANC) has been widely researched to reduce engine, intake or exhaust, and road noise in passenger cars [1]–[4]. In particular, ANC for the suppression of engine noise has been actively applied to mass-produced vehicles. Using ANC to suppress road noise has also been actively researched for mass production over the past decade [4] and recently adopted [5], [6] because ANC can efficiently attenuate low-frequency noise without significant structural modification or additional weight increases. In an early study of ANC for engine noise, Elliott and Nelson [7] presented an active control system to suppress the engine firing order. They used four microphones and two speakers to achieve global noise attenuation. Their system realized a noise attenuation of approximately 10 to 15 dB for an engine firing order within engine revolution speeds of 3,500-6,000 revolutions per minute. Using ANC for engine noise suppression has continued to be researched by developing more sophisticated adaptive signal processing algorithms, digital signal processing (DSP) systems, and digital sensors [8]. Sophisticated algorithms for fast convergence speed, incredible noise attenuation performance, and improved stability have been proposed [9]–[13]. Fast affine projection algorithms based on the Gauss-Seidel solving scheme or the dichotomous coordinate descent method deliver promising options to increase the robustness and reduce the computational cost [14], [15]. Moreover, low-cost but high-performance DSP hardware allows ANC to be implemented in mass-production vehicles [16], [17].

In a modern vehicle active control system for engine harmonics, the engine revolution speed has been used as a reference signal to generate a harmonic signal of the corresponding engine order frequency instead of microphones or accelerometers. The engine firing order can be effectively controlled using an adaptive notch filter [18]. Likewise,

The associate editor coordinating the review of this manuscript and approving it for publication was Yingxiang Liu.

engine harmonic and subharmonic orders can be effectively controlled using an adaptive notch filter [19]. The engine speeds can be obtained via a high-speed controller area network (CAN) bus [20]. Schirmacher *et al.* [21] presented the practical implementation of active noise control to deal with cylinder deactivation. In their system, the engine revolutions/minute (RPM) was picked up and used as a reference signal instead of physical sensors such as microphones or accelerometers, and the engine firing order was effectively controlled in the 4-cylinder mode and the 8-cylinder mode of the 8-cylinder engine. Likewise, many studies have attempted to reduce the interior or exterior noise of exhaust systems [19], [22]. The active control system for suppressing the exhaust noise also picks up the engine speed and generates a reference signal similar to the ANC system for engine noise since exhaust noise is also directly linked to engine speed.

Although, many studies have been presented on the active control of engine harmonics and exhaust noise. However, studies or practical attempts regarding the active cancellation of driveline noise are scarce. One of the reasons may be that additional reference sensors are required since the frequency of the driveline noise does not have a harmonic relationship with the engine rotation signal. Another reason is that there has been no study or attempt to generate a reference signal without employing the physical sensor. Thus, most studies have used a passive approach to improving driveline noise [23]–[25]. As a traditional noise, vibration, and harshness (NVH) approach for driveline noise, noise and vibration were improved through the optimal design of the propeller shaft focused on its alignment and balancing [26]–[28]. Kim [28] investigated the reduction of driveline vibration during rapid acceleration by improving the alignment angle of the propeller shaft of a rear-wheel drive vehicle. In his study, the alignment angle of the propeller shaft, which was determined considering only the constant speed driving condition, was improved by considering the rapid acceleration driving condition as well as the constant speed driving condition. As a result of the optimization, the angular velocity fluctuation was 0.025% after the improvement, whereas it was 0.150% before the improvement. Meanwhile, the imbalance which is generally occurred by runout in the rotating parts of the drive system is generally managed through design perspective [29]. Moreover, Steyer [26] proposed modal mapping strategies for driveline systems based on finite element analysis (FEA). To achieve the overall NVH performance of the driveline, a strategy for determining the specifications of each part at the component level, such as the mounting location, bushing rates, modal property of the propeller shaft, and dynamic characteristics of the joint, was presented. Meanwhile, there have also been attempts to install various liners on the propeller shaft tube to reduce vibration in the driveline. The liner treatment may provide damping to the driveline system to reduce vibration amplitude [30].

Although passive methods are relatively effective for noise reduction, they have limitations, such as the fact that they are costly, cause weight increments, and can be effective only in a limited frequency range. It is not only the engine noise but also the booming noise caused by the driveline that are significant factors in interior noise during acceleration. Therefore, an active approach to improve the limitations of the conventional passive method is required.

To address these limitations, we propose a method to suppress driveline noise, such as propeller shaft noise and tire noise, with an active approach without employing physical reference sensors. The primary aim of this study is to design an active control algorithm that can suppress not only engine firing order but also driveline noise, which is nonharmonic with engine speed. Furthermore, the performance of the proposed algorithm was evaluated through the practical implementation of the active control system. This paper is organized as follows. Section 2 presents the driveline NVH phenomenon. In Section 3, the control algorithm to suppress the engine firing order and driveline noise, which is the nonharmonic relation with engine order, is presented. Section 4 describes the implementation of a control system for the vehicle. Section 5 presents the experimental results. Finally, the conclusions of this work are presented in Section 6.

II. NVH PHENOMENON IN THE DRIVELINE

A front-engine and front-wheel drive (FF) vehicle has an engine and transmission located in the front of the vehicle. The engine and transmission are mainly transversely connected, and the power from the transmission is transmitted to the front wheels through the drive shaft. Meanwhile, a front-engine and rear-wheel drive (FR) vehicle mainly has an engine and transmission connected in a longitudinal direction, and power from the transmission is transmitted to the rear wheels through a propeller shaft. The propeller shaft transmits power to the differential at the shift output stage. The drive shaft delivers torque from the transmission to the wheels. The transfer divides the power of the front and rear wheels, and the differential gear controls the revolution speed between the left and right driving wheels by evenly distributing the torque and the revolution speed. In the case of FR vehicles, it is easy to cope with high power, and it is advantageous for dynamic drivability. However, they are more sensitive to the low-frequency vibration of the powertrain than FF vehicles. In an FF all-wheel drive (AWD) vehicle, power is delivered to the rear wheels using a transfer and propeller shaft. Meanwhile, in an FR AWD vehicle, power is diverted from the transfer located at the end of the transmission and delivered to the front wheels. The transfer withdraws the driving force, and the coupling functions distribute the driving force. The transfer and coupling functions are separated in an FF vehicle, but an FR vehicle includes a coupling function inside the transfer. Figure 1 illustrates the overall layout and power transfer flow for the driveline of FF and FR AWD vehicles. The abbreviations indicated in Fig. 1 are as follows: engine (Eng), transmission (T/M), drive shaft (D/Shaft), differential (Diff), propeller shaft (P/Shaft). Moreover, Fig. 1 (a) and (b) indicate the layouts of FF and FR
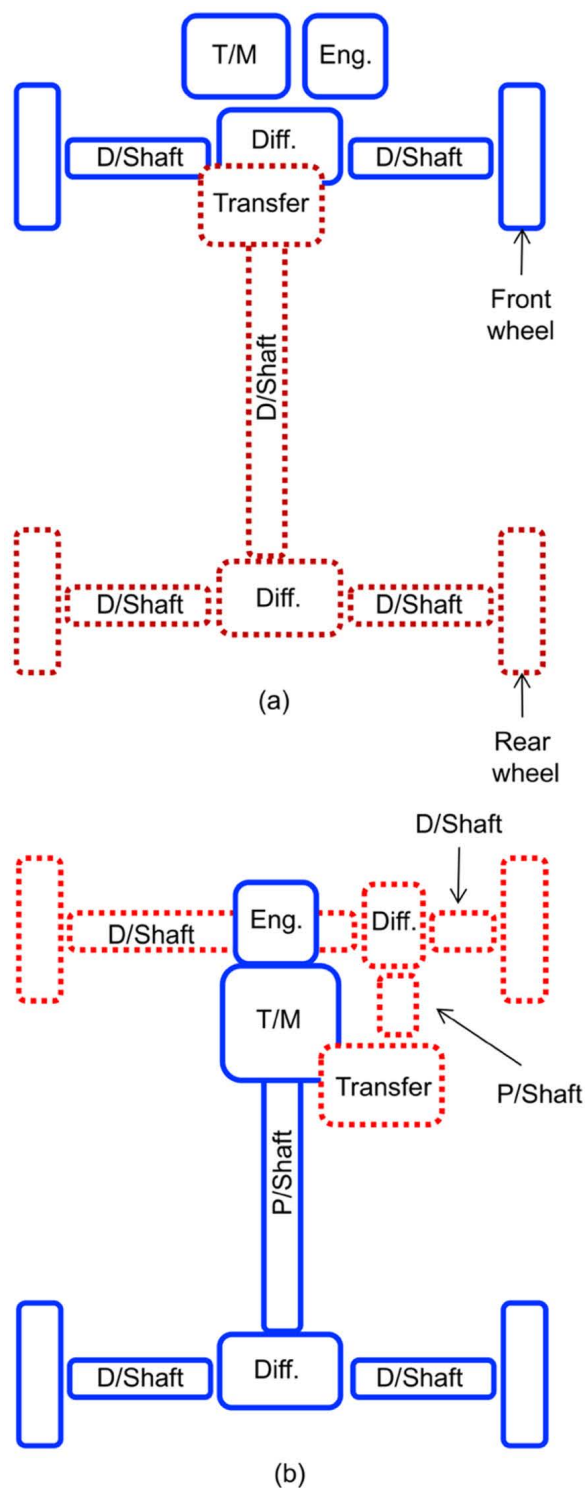
FIGURE 1. The overall layout and power transfer for the driveline of FF and FR AWD vehicles. (a) The driveline of the FF vehicle and (b) the driveline of the FR vehicle.

vehicles, respectively. In Figure 1, the blue rectangle indicates the power transmission flow discharged from the powertrain, and the red dotted rectangle indicates the power transmitted to other wheels.

The primary causes of NVH problems in the driveline are torque fluctuations due to improper joint angle of the

driveline and imbalance in rotating parts. Torque fluctuations and imbalance act as excitation forces and resonate with the natural frequency of the torsional mode and bending mode of the driving shaft or with the rigid body mode of the driveline and are transmitted to the vehicle body. Therefore, the driveline NVH may be considered from an excitation source perspective and a transfer path perspective. First, the NVH problem for each driveline part due to the excitation source is as follows.

- Powertrain: Vibration and noise of engine and transmission
- Drive shaft: Excitation force due to the structure of the constant velocity joint during rotation
- Propeller shaft: Vibration generated by angular velocity change according to the bending angle of the coupling part, excitation force due to imbalance
- Differential: Vibration and noise caused by gear engagement
- Tire: Excitation force due to tire rotation

Next, NVH problems due to the transfer path are as follows.

- Powertrain: Resonance with elastic mode
- Drive shaft: Resonance in shaft bending mode
- Propeller shaft: Shaft bending, torsional, and vertical mode
- Differential: Resonance of the case, rigid body mode of the differential, mode coupling with the rear crossmember

Typical excitation forces of the rear-wheel-drive system include the imbalance of the rotating part of the driveline and torque fluctuations due to the improper joint angle of the driveline. It is challenging to set the optimum angle arrangement of the driveline in a way that satisfies all the various driving conditions, such as rapid and slow acceleration/deceleration [28]. Therefore, the driveline in which the bending angle is formed has different joint angles on the drive shaft, thereby causing an angular velocity fluctuation of the propeller shaft. A constant velocity joint can be used to eliminate the difference in angular velocity due to the alignment angle arrangement of the drive shaft which can improve the vibration of the driveline [28]. However, it is mainly applied to high-end vehicles due to its relatively high cost. Meanwhile, when the excitation force amplified by the torque fluctuation of the driveline resonates with the natural frequency of the torsion mode or bending mode of the drive shaft or the rigid body mode of the driveline [30], vibration is transmitted to the vehicle body, resulting in vibration and booming noises in the vehicle interior. To improve such resonance problems, various studies have been conducted to separate the natural frequencies of the driveline [31], [32]. However, this may adversely affect vibration in other driving regions due to the shift of the natural frequency [30].

Since there are limitations to the passive approach for mitigating driveline noise, this study focused on using active control to suppress the propeller shaft noise. Moreover, tire noise corresponding to the tire rotation frequency was also considered.
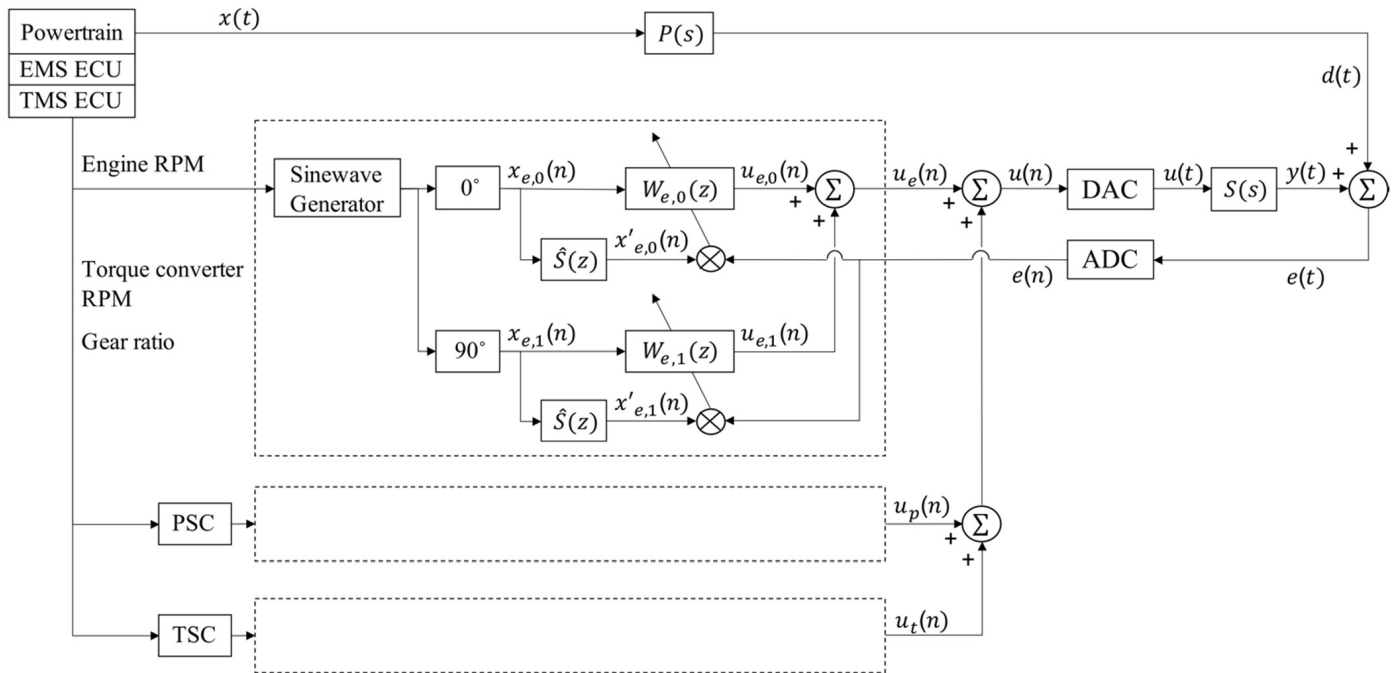
FIGURE 2. Block diagram of the FxLMS for control of the engine harmonic and driveline noise.

However, since the propeller shaft and tire rotation noise are not harmonic components of the engine speed, the conventional method using the engine speed as a reference signal cannot be applied. Therefore, in this study, we propose a novel method that generates a reference signal for driveline noise control by calculating the rotational speeds of the propeller shaft and tires from the engine speed. The proposed algorithm in this study is outlined in Section 3.

III. THEORETICAL CONSIDERATION

If the primary noise is periodic noise with a sinusoidal component, a sinewave signal can be used as a reference signal to cancel narrowband noise. When sine waves are utilized as reference signals, the least mean square (LMS) algorithm takes the form of an adaptive notch filter [18]. Thus, an adaptive notch filter based on the filtered-x LMS (FxLMS) algorithm has mainly been used for active control of engine noise [33]. Moreover, a number of sinewaves may be configured as reference signals to control not only the engine firing order but also its harmonic components. In practice, to control the firing order and the harmonic component, the engine speed is used to generate a corresponding sinewave. However, for driveline noise control, such as propeller shaft and tire noise, engine speed cannot be used as a reference signal because their rotational speed, which varies according to the gear shift stage, is not a harmonic of engine rotational speed. Therefore, this study proposes a new method for generating reference signals for the propeller shaft and tire noise from engine speed to control the driveline noise. Figure 2 illustrates a block diagram of a narrowband FxLMS algorithm. In Fig. 2,

each dashed rectangle represents the adaptive notch filter corresponding to the engine noise, propeller shaft noise, and tire noise.

In Fig. 2, $x(t)$ is the reference signal, $d(t)$ is the disturbance signal, $u(t)$ is the control signal, $y(t)$ is the output signal in the secondary path, and $e(t)$ is the error signal. $P(s)$ and $S(s)$ imply the primary path and secondary path, respectively, and $\hat{S}(z)$ is the estimated model of the secondary path. t is a continuous-time variable, and s denotes a continuous complex operator. $x(n)$ is the discrete form of $x(t)$ and is a pure sine wave [33].

$$x(n) = x_o(n) = Asin\left(\omega_0 \frac{n}{f_s}\right) \tag{1}$$

where A is the amplitude, n is the discrete time variable, and f_s is the sampling frequency. The sampling frequency was 6,400 Hz. The 90° phase-shifted function can be used to generate the quadrature reference signal

$$x_1(n) = Acos\left(\omega_0 \frac{n}{f_s}\right) \tag{2}$$

For engine harmonic control, ω_0 can be directly obtained from the engine rotational speed and expressed as follows.

$$\omega_0 = 2\pi \frac{N_e}{60} \tag{3}$$

where N_e is the engine speed, which can be represented in RPM. Thus, the reference signal for engine noise, $x(n)$, can be expressed as follows.

$$x(n) = Asin\left(2\pi \frac{N_e}{60} \frac{n}{f_s}\right) \tag{4}$$

For engine harmonic control, multiple sinusoidal components can be used. Accordingly, a harmonic component, k, is added to the reference signal for the engine harmonic order as in equation (5). Since the firing order of the six-cylinder engine is the third order, k becomes 3.

$$x_e(n) = A sin\left(2\pi \frac{N_e}{60} k \frac{n}{f_s}\right) \qquad (5)$$

Meanwhile, since the engine speed cannot be directly used for propeller shaft and tire noise control, the reference signals are generated by calculating the speed of the driveline as follows.

$$x_p(n) = A sin\left(2\pi \frac{N_{tc}}{60 R_{gear}} k \frac{n}{f_s}\right) \qquad (6)$$

$$x_t(n) = A sin\left(2\pi \frac{N_{tc}}{60 R_{gear} R_{finaldrive}} k \frac{n}{f_s}\right) \qquad (7)$$

where N_{tc} is the RPM of a torque converter and R_{gear} and $R_{final\,drive}$ represent the gear ratio and final drive ratio, respectively. In Fig. 2, the PSC and TSC represent the propeller shaft speed calculator and tire speed calculator derived from equation (6) and equation (7).

Each reference signal passes through the estimation of the secondary path, $\hat{S}(z)$, and becomes $x'(n)$ [18].

$$x_0'(n) = \sum_{i=0}^{L-1} \hat{S}_l(n) x_0(n-l) \qquad (8.1)$$

$$x_1'(n) = \sum_{i=0}^{L-1} \hat{S}_l(n) x_1(n-l) \qquad (8.2)$$

where $\hat{S}_l$ is the lth coefficient of the impulse response function (IRF) of $\hat{S}(z)$ and L is the length of the IRF of $\hat{S}(z)$. $\hat{x}_0(n)$ and $\hat{x}_1(n)$ are used to update the coefficient of the control filter. The coefficient vector of the control filter, $W(z)$, is expressed as follows.

$$\mathbf{w}(n) = [w_0(n), w_1(n)]^T \qquad (9)$$

Thus, the updated equation of the adaptation algorithm is given as [34].

$$\mathbf{w}(n+1) = \mathbf{w}(n) - \alpha \mathbf{x}'(n) e(n) \qquad (10)$$

where α is a convergence coefficient and $\mathbf{x}'(n)$ is a filtered reference signal vector that passed through the secondary path model.

IV. IMPLEMENTATION OF THE ACTIVE NOISE CANCELLATION SYSTEM

Next, this real-time adaptive controller was implemented for a six-cylinder large FR AWD sedan with an eight-speed automatic transmission to evaluate noise suppression performance. Figure 3 shows the overall schematic representation of the active noise control system. Four microelectromechanical system (MEMS)-type microphones (SPG08P4HM4H-1, Knowles) were used for measuring error signals and were installed on the headliner, one for each seat. The microphones were connected to the controller through an automotive audio
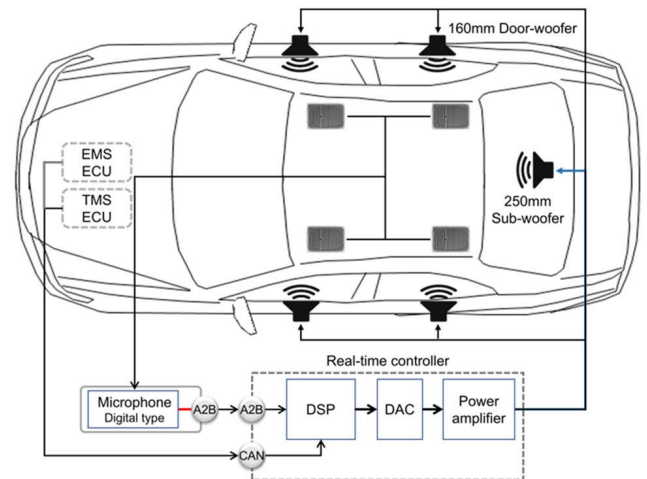

FIGURE 3. Overall schematic representation of the active noise control system.
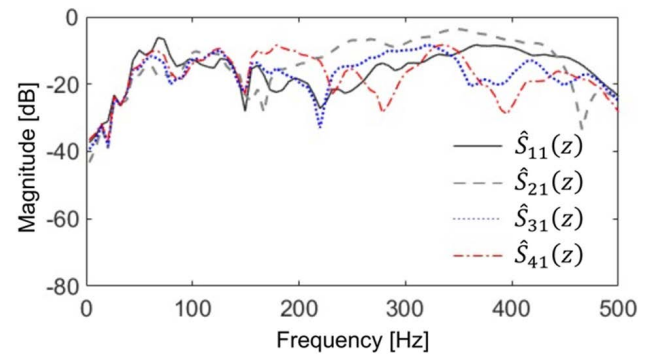

FIGURE 4. Magnitude plot of the frequency response function for the estimated secondary path model.

bus (A2B) interface (AD2425, ANALOG DEVICES). Four door loudspeakers and one subwoofer (illustrated in Fig. 3) were used as secondary sources to cancel the primary noise inside the vehicle. The secondary path was estimated by the offline identification method. Figure 4 shows the magnitude of the frequency response function for the estimated secondary path model between the front left door-woofer and each microphone. In Fig. 4, the black solid, gray dashed, blue dotted, and red dashed-dotted lines indicate the estimated secondary path model $\hat{S}_{11}(z)$ between the front left error microphone and the front left door-woofer, $\hat{S}_{21}(z)$ between the front right error microphone and the front left door-woofer, $\hat{S}_{31}(z)$ between the rear left microphone and the front left door-woofer, and $\hat{S}_{41}(z)$ between the rear right microphone and front left door-woofer, respectively. The RPM of the engine and torque converter and the information about the gear stage were obtained from the engine management system electronic control unit (EMS ECU) and transmission management system electronic control unit (TMS ECU) via a high-speed CAN bus. CAN with a flexible data rate (FD) was used as a protocol to reduce latency. Moreover, the real-time
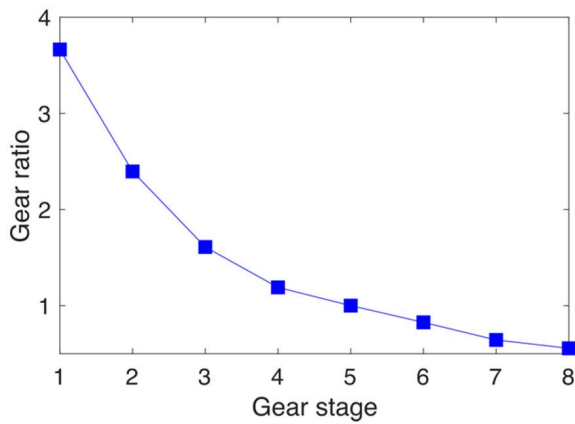
FIGURE 5. The gear ratio of the test vehicle.

FIGURE 6. Measurement microphone positions for evaluating the noise attenuation performance.

controller was implemented on the DSP with an audio amplifier. The DSP was employed the DRA 751 Jacinto 6 (Texas Instruments), which has two 750 MHz C66x DSP. The sampling frequency was 6,400 Hz, and the frequency range of ANC was approximately 20-300 Hz.

Figure 5 shows the gear ratio of the test vehicle. The final drive ratio is 3.909. The engine firing order (C3), the first order of the propeller shaft (P1), and the second (T2) and third (T3) orders of the tire, which are related to the final drive gear, were considered the targets of active cancellation.

V. EXPERIMENTAL RESULTS AND DISCUSSION

The noise attenuation performance of the proposed algorithm was evaluated, and its experimental results are discussed in this section. The ANC experiment was conducted for every seat position of a passenger car. The interior sound pressure level was measured using a 1/2-inch microphone in eight locations, i.e., both left and right ear positions of each seat, as shown in Fig. 6. The interior noise was measured during a wide-open throttle in the sixth gear since the rotation speed of the driveline is low while in low gear. The spectrograms before and after control in the driver's and rear right seats are illustrated in Fig. 7. Before control, as shown in Fig. 7 (a) and (b), the tonal noise of the C3 and P1 orders is high for both the driver's seat and the rear seat, but the noise level at the rear seat was higher than that of the driver's seat. Moreover, for orders T2 and T3, the driver's seat was slightly higher than the rear seat. However, as illustrated in Fig. 7 (c) and (d), the tonal noise of C3 and P1 was dramatically suppressed due to ANC. In addition, the T2 and T3 orders were also effectively suppressed for both the driver and the rear seats.

The experimental results before and after control according to each rotation speed are presented in more detail in Figs. 8 to 11, where the dashed gray and solid blue lines indicate the C-weighted sound pressure level before and after ANC, respectively, with regard to engine speed. First, the result for the C3 order is illustrated in Fig. 8. The C3 order was attenuated by up to 20 dB after control. A slight overshoot
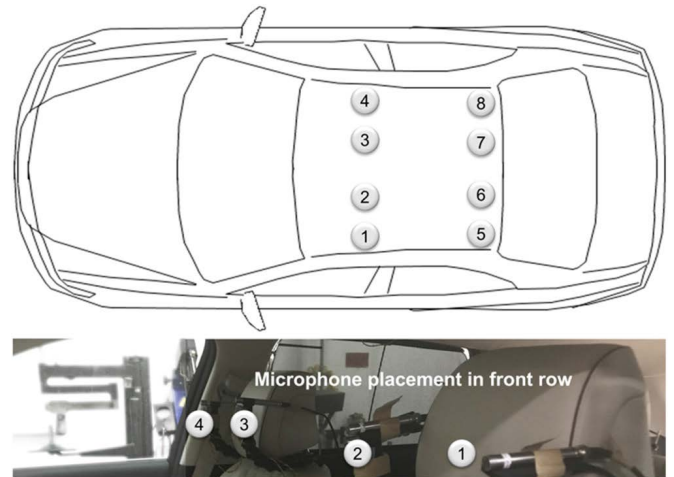
occurred at approximately 1,250 RPM and 2,800 RPM in the driver's seat right ear position. A similar overshoot occurred at 1,600 RPM in the left ear of the rear right seat. It is estimated that the control stability was somewhat degraded at the ear positions in the center of the vehicle cabin because error microphones were located at the window-side position of the cabin. Although a slight overshoot has been found in some regions, the overall engine booming noise has been effectively suppressed by the ANC.

Next, the result for the P1 order is illustrated in Fig. 9. The P1 order was attenuated by up to 15 dB after control. Both the low-speed booming noise that occurred at 1,500 RPM and 2,300 RPM in the driver's seat and the booming noise at 2,700 RPM and 2,800 RPM in the rear right seat position were effectively suppressed. In particular, the noise suppression performance was higher in the rear seat position than in the driver's seat position. Finally, the results for the T2 and T3 orders are illustrated in Fig. 10 and Fig. 11. The T2 and T3 orders were attenuated by up to 10 dB after control. An overshoot of the T2 order was found at approximately 550 RPM and 950 RPM at the left ear position of the rear right seat.

Since the frequency corresponding to the rotation speed of the T2 order is less than approximately 20 Hz, performance degradation is considered to have occurred due to the limitation of the control speaker. Although an overshoot has been observed in some RPM ranges, it can be confirmed that tire noise is also sufficiently suppressed overall through ANC.

Table 1 presents the C-weighted SPL of the C3, P1, T2, and T3 orders before and after ANC at all microphone positions. Furthermore, a comparison of the noise attenuation of each control target for each measurement position is shown in Fig. 12. For the C3 order, the average attenuations from 1,100 to 3,200 RPM were 8.9 dB, 6.7 dB, 5.9 dB, 7.3 dB, 13.0 dB, 7.0 dB, 4.7 dB, and 10.4 dB at the positions of the left and right ears of the driver, front passenger, rear left, and rear right seats, respectively. The engine booming noise of the C3 order was effectively suppressed to 4.7 dB from a
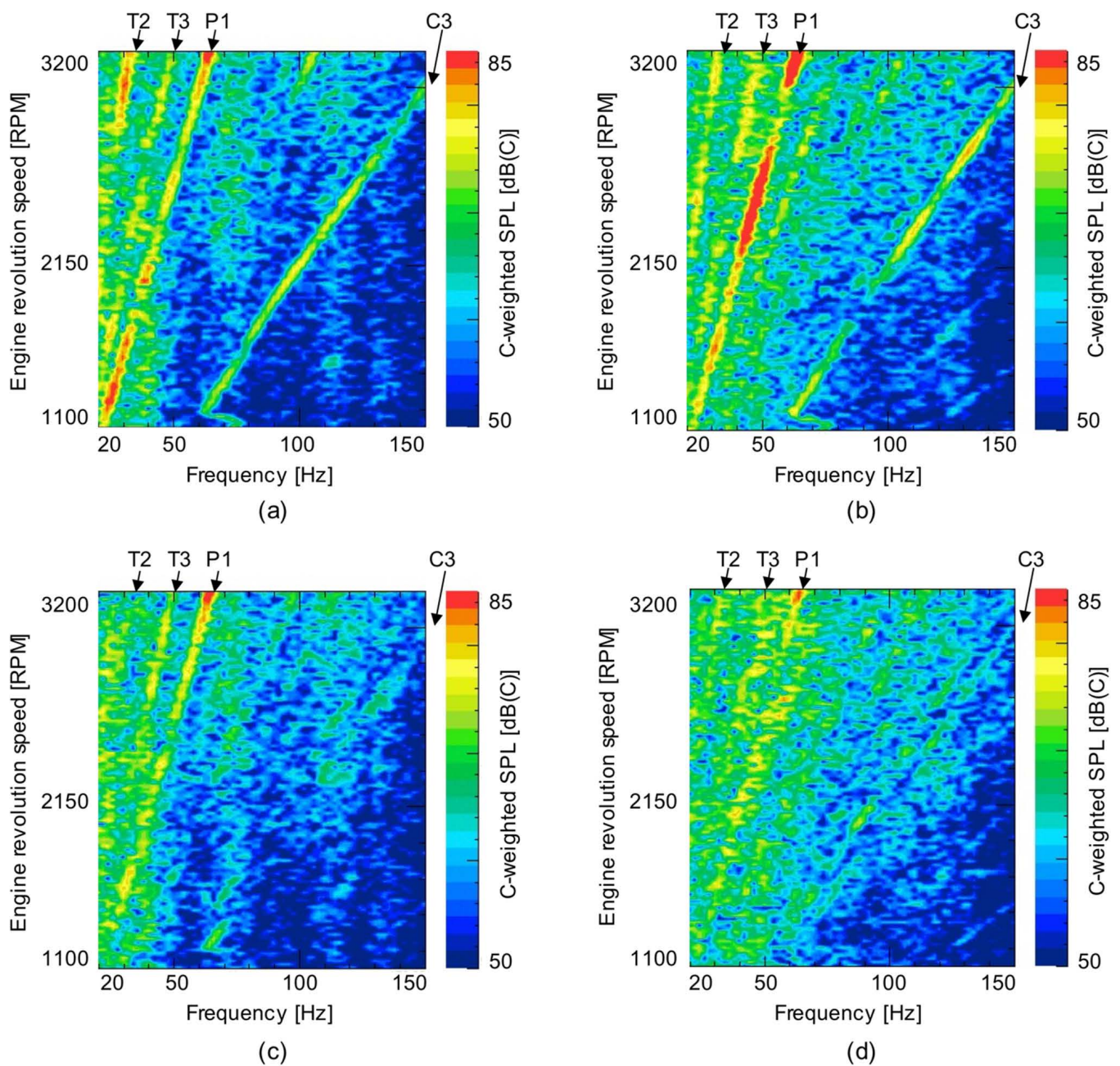
FIGURE 7. C-weighted sound pressure level at the driver and rear passenger position according to control. (a) Before control at the front left position, (b) before control at the rear right position, (c) after control at the front left position, (d) after control at the rear right position.

maximum of 13.0 dB, with an average attenuation of 8.0 dB for all seat positions. Next, for the P1 order, the average attenuations from 1,370 to 3,800 RPM were 2.4 dB, 5.1 dB, 5.5 dB, 3.4 dB, 6.0 dB, 7.4 dB, 6.7 dB, and 7.8 dB at the positions of the left and right ears of the driver, front passenger, rear left, and rear right seats, respectively. An average attenuation of 5.5 dB was found for all seat positions. The P1 order is also effectively controlled, similarly to the C3 order.

Finally, for the T2 order, the average attenuations from 330 to 990 RPM were 6.8 dB, 5.1 dB, 4.4 dB, 6.3 dB, 3.5 dB,

1.4 dB, 1.0 dB, and 2.9 dB, and for the T3 order were 3.5 dB, 2.9 dB, 0.6 dB, 0.2 dB, 1.4 dB, 1.8 dB, 4.0 dB, and 3.6 dB at the position of the left and right ear of the driver, front passenger, rear left, and rear right seats, respectively. The average attenuation of all seat positions was 3.9 dB for the T2 order and 2.3 dB for the T3 order. For the T3 order, the noise suppression performance at the rear left passenger position (microphones 3 and 4) was relatively insufficient. It is expected that if the position of the poorly performing microphone is optimized, then the performance will be improved.
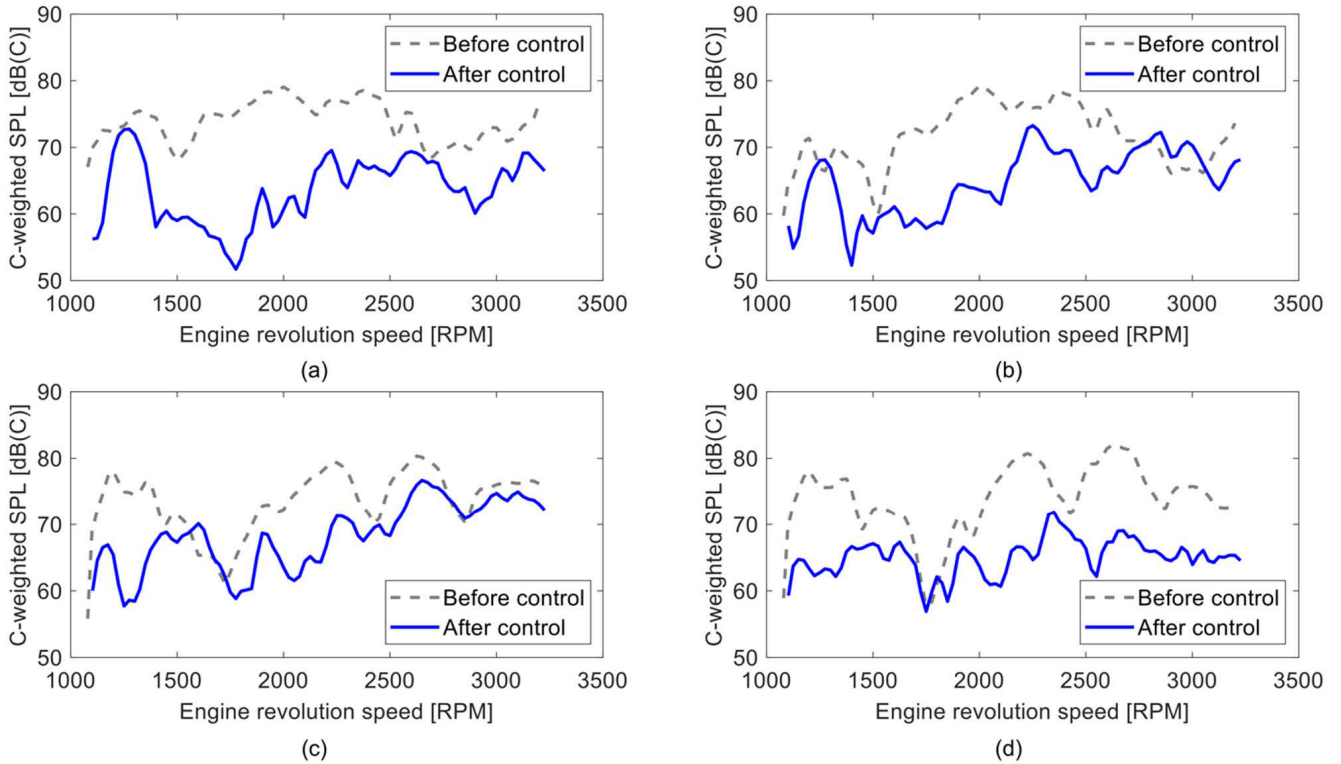
FIGURE 8. Noise attenuation performance for the C3 order according to measurement positions. (a) The left ear of the driver seat, (b) right ear of the driver seat, (c) left ear of the rear right seat, (d) right ear of the rear right seat.

FIGURE 9. Noise attenuation performance for the P1 order according to measurement positions. (a) The left ear of the driver seat, (b) right ear of the driver seat, (c) left ear of the rear right seat, (d) right ear of the rear right seat.
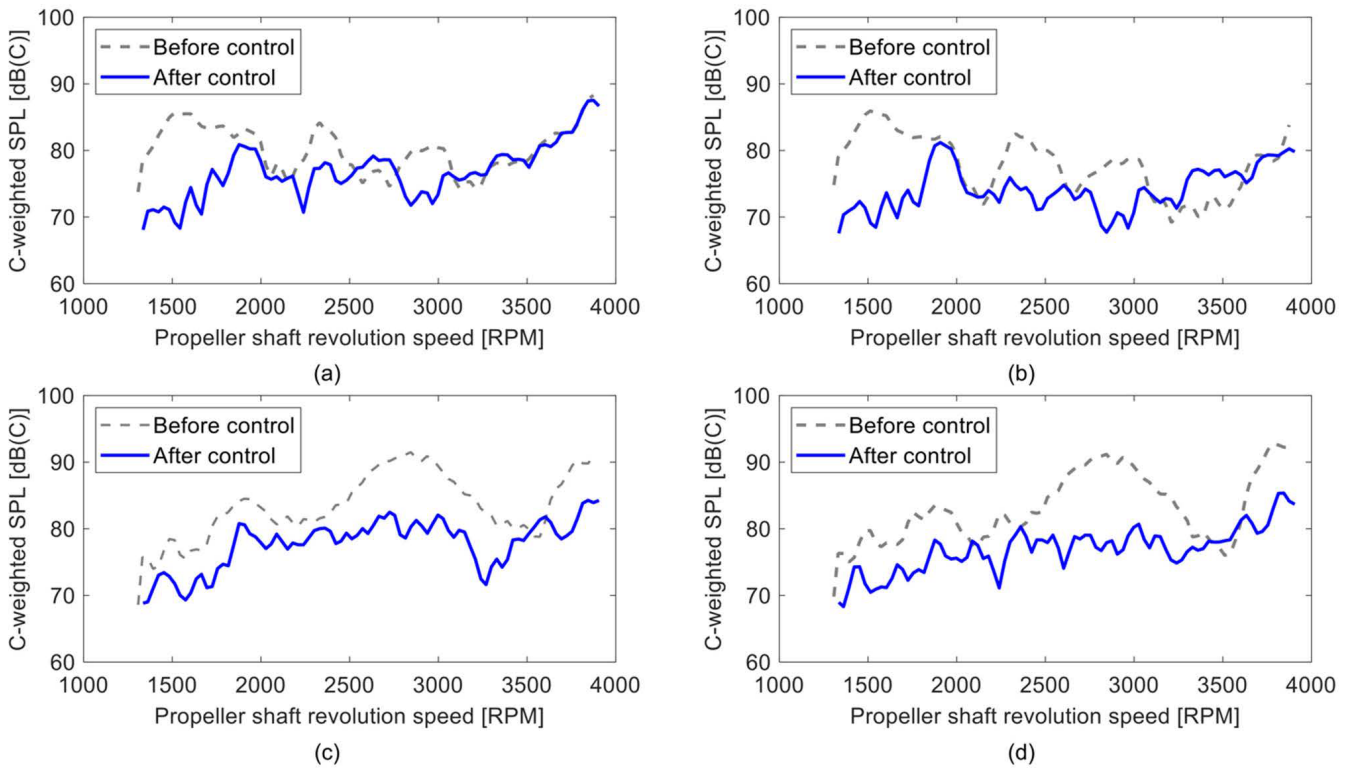
The active control of the engine firing order can be considered effectively suppressed, similarly to previous research results [3]. Moreover, the driveline noise was also effectively suppressed as well as the engine noise with the
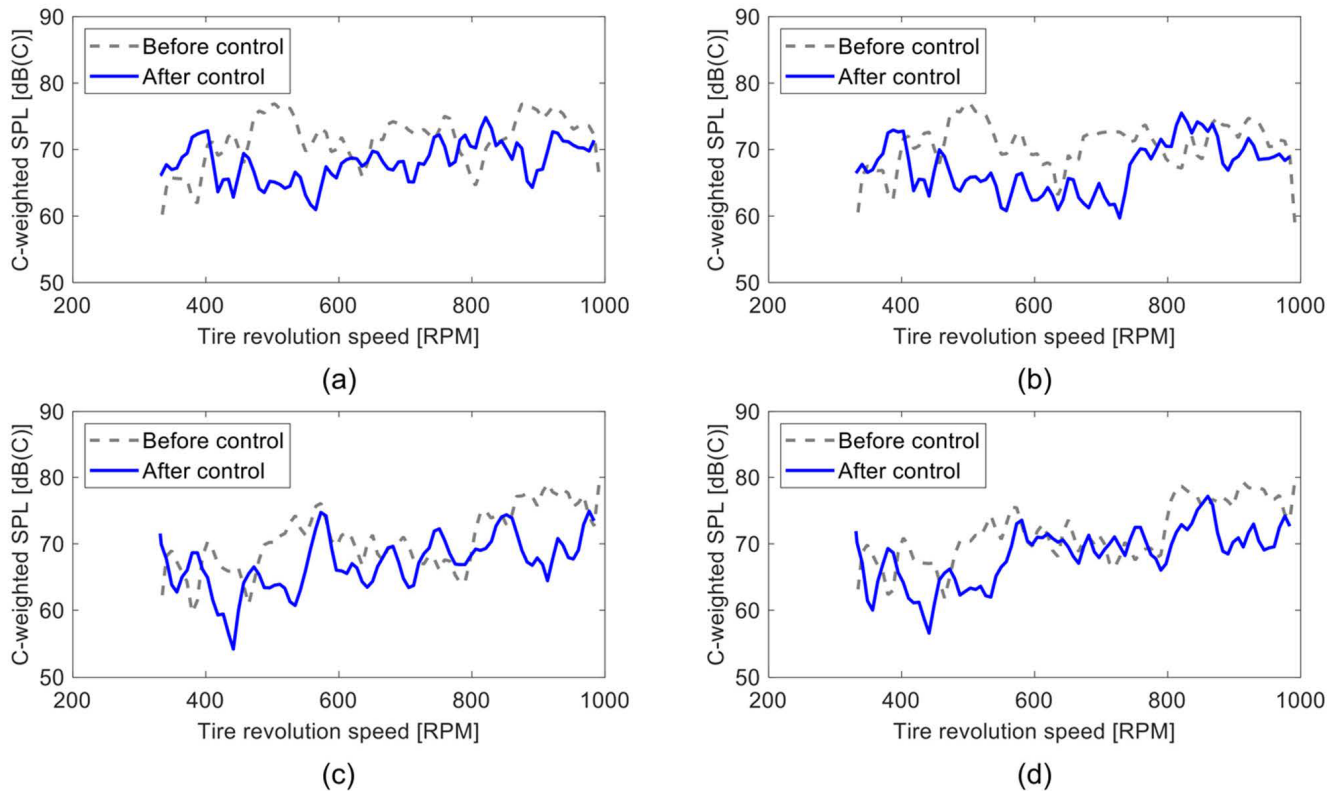
FIGURE 10. Noise attenuation performance for the T2 order according to measurement positions. (a) The left ear of the driver seat, (b) right ear of the driver seat, (c) left ear of the rear right seat, (d) right ear of the rear right seat.

FIGURE 11. Noise attenuation performance for the T3 order according to measurement positions. (a) The left ear of the driver seat, (b) right ear of the driver seat, (c) left ear of the rear right seat, (d) right ear of the rear right seat.
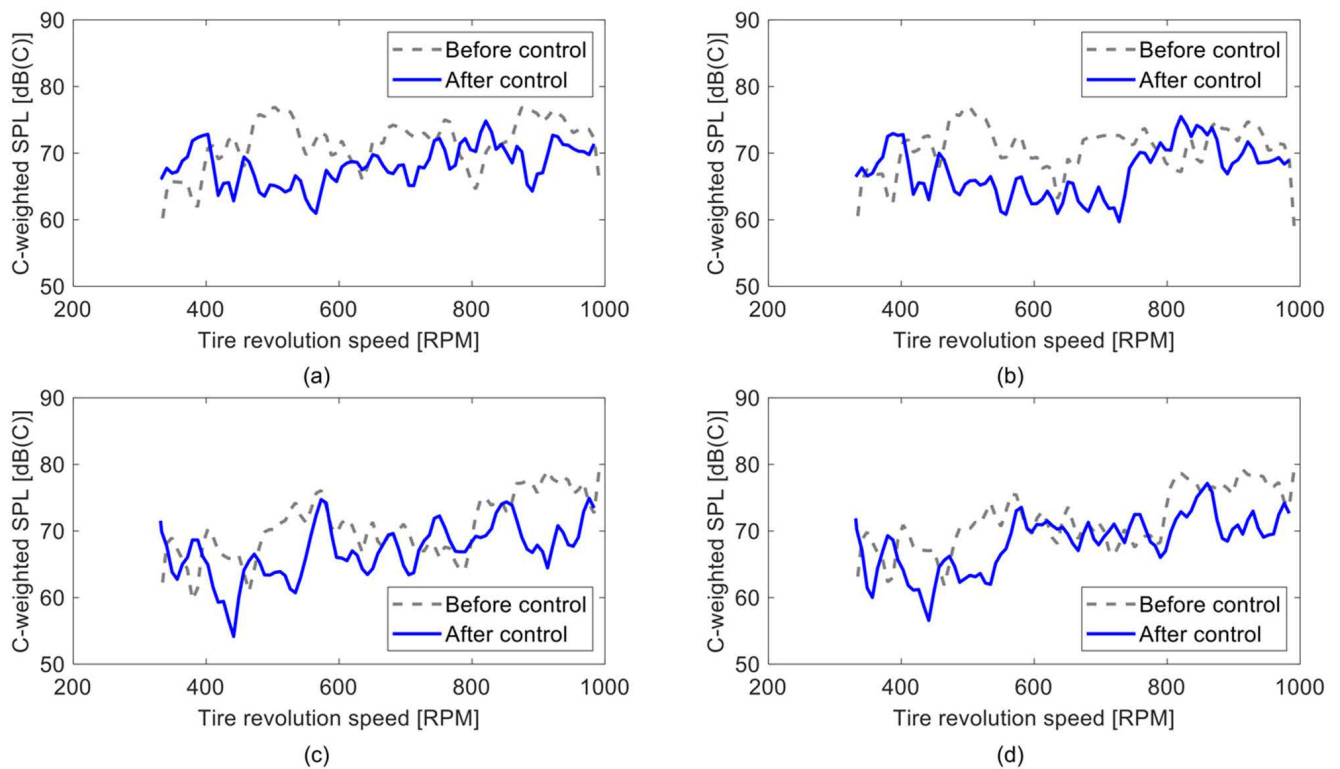
proposed method. Therefore, it can be considered that the proposed method is effective in suppressing driveline noise.

However, few studies in the literature have attempt to find an active method of reducing driveline noise. Thus, the

TABLE 1. C-weighted sound pressure level according to ANC (F-Front, B-Back, L-Left, R-Right).

|	C-weighted sound pressure level [dB(C)] by measurement position							
Category	FL left ear	FL right ear	FR left ear	FR right ear	BL left ear	BL right ear	BR left ear	BR right ear
				Before control				
C3	74.85	73.75	73.16	73.83	75.89	75.36	75.33	76.23
P1	81.46	79.83	79.46	81.84	84.75	85.93	85.84	86.06
T2	76.08	73.26	71.38	74.95	73.92	72.24	71.62	73.38
T3	72.77	71.80	69.94	71.68	73.18	72.26	72.83	73.67
				After control				
C3	65.93	67.05	67.30	66.53	62.96	68.37	70.65	65.88
P1	79.04	74.76	73.94	78.49	78.78	78.54	79.14	78.30
T2	69.24	68.13	66.95	68.67	70.43	70.82	70.62	70.53
T3	69.23	68.87	69.32	71.48	71.81	70.42	68.85	70.10
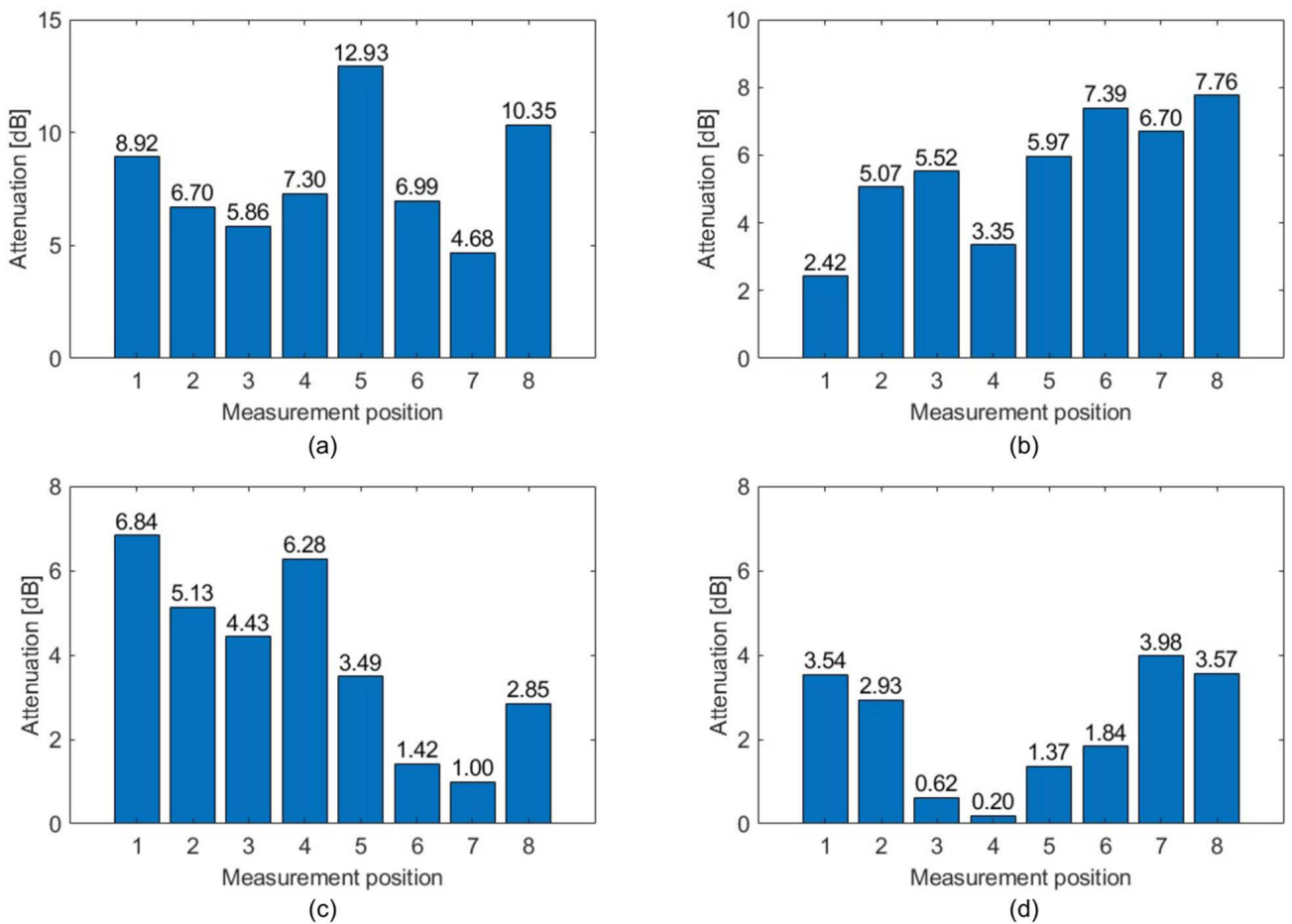
FIGURE 12. Comparison of noise attenuation by the ANC target category according to the measurement position. (a) Attenuation of the C3 order, (b) attenuation of the P1 order, (c) attenuation of the T2 order, (d) attenuation of the T3 order.

effectiveness of the driveline noise reduced by the active method is compared with conventional passive methods. For driveline NVH issues, there are many attempts to reduce the vibration directly. Becker *et al.* [35] presented experimental results that reduce the first-order booming noise by controlling the imbalance of the driveline. They show a 10 dB reduction in the interior noise at a constant driving speed of 62 mile/h by adjusting the looseness of the plunger of
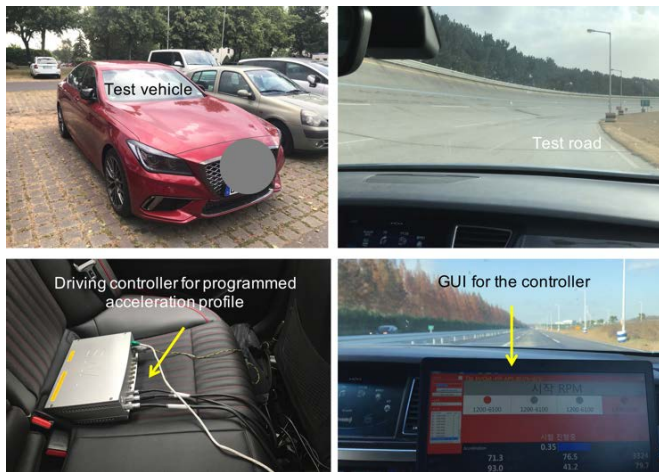
FIGURE 13. Experimental setup for the subjective evaluation of annoyance perception according to noise attenuation.

that the NVH of the driveline can be more effectively improved.

VI. SUBJECTIVE EVALUATION

Following the objective evaluation, a subjective evaluation was also conducted to evaluate the perception of noise suppression performance. Fifteen subjects (male: 13, female: 2) between 29 and 52 years old (median: 38) with normal hearing ability who had background knowledge about acoustics and vehicle NVH participated in the experiment. The participants understood the purpose of the evaluation before the test, and they participated in the evaluation after submitting written consent. Figure 13 illustrates the experimental setup for the subjective evaluation.
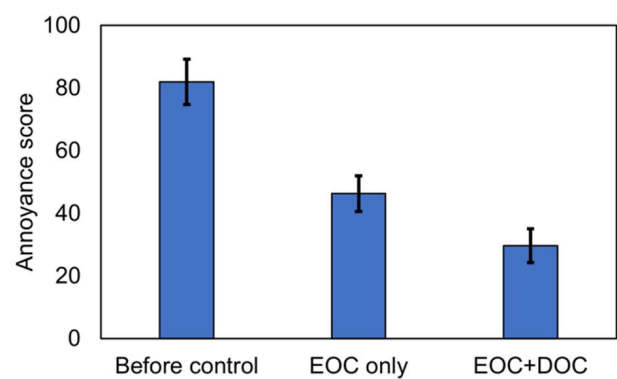

FIGURE 14. The evaluation result of the annoyance rating according to active control.

the propeller shaft. Britto *et al.* [36] presented the effect of adding mass and dynamic dampers on the interior noise. To reduce the booming noise induced by the vibration mode of the driveline, they evaluate the addition of a mass and dynamic damper to the drive shaft. In their study, the interior noise is reduced by 3.0 dB in the range of the booming noise by attaching an additional mass of 1 kg to the drive-shaft. Moreover, it was shown that the interior noise was reduced by 3.3 dB by installing a dynamic damper. Likewise, Vikram *et al.* [37] propose the dual degree of freedom vibration damper (DDVD) to reduce the vibration due to the propeller shaft bending mode and compare the performance with the conventional torsional vibration damper (TVD). Dynamic dampers are installed on the rear axle side flange of the propeller shaft. When evaluating the noise reduction effect in the rear passenger position, the DDVD shows the booming noise mitigation at both low speed and high speed, whereas the TVD shows the effectiveness only at low speed. Moreover, subjective rating showed that the scores of the DDVD were improved from 5 to 7 points at low engine speed and 6 to 7 points at high engine speed, whereas the TVD was improved from 5 to 7 points at low engine speed. Although the dynamic damper can be applied to reduce the vibration of the driveline and the interior noise caused by it, the impact is limited to a narrow frequency range.

Since the evaluation vehicle and conditions are not the same as those of previous studies, it is difficult to compare noise attenuation directly. However, it is considered that the active control approach of the driveline noise proposed in this study shows better noise reduction performance than the conventional passive method. Moreover, the passive approach, such as mass and dynamic dampers, are only effective at limited frequency, whereas the active approach can reduce noise in a broad frequency region. Although interior noise can effectively be suppressed through active noise control, the limitation of continuing source vibration remains.

Therefore, if the passive method and the active method proposed in this study are combined, it is expected

The subjects drove the evaluation track on their own and rated the annoyance before and after control under a wide-open throttle condition in the sixth gear where significant booming noise was observed. As the subjects drove themselves, there may have been differences in the perception of interior noise according to the difference in acceleration profiles for each subject. To prevent this experimental error, the same acceleration pattern was implemented regardless of the accelerator pedal trajectory using a driving controller. In the test, the Rohrmann scale [38] was applied to rate the annoyance. Equidistant verbal anchors such as not at all (0), a little (25), moderately (50), quite slightly (75), and extremely (100) were used. Three experiments, namely before control, only engine order control (EOC), and simultaneous control, which is combined with EOC and driveline order control (DOC), were conducted to compare the perceptual annoyance. Figure 14 shows the mean and 95% confidence interval of the assessed annoyance scores. The annoyance score before the control averaged 82 points (standard deviation (SD) 14.2). When EOC was applied, the annoyance score decreased by 35.7 to 46.3 points (SD 11.3). Moreover, it was found that when simultaneous control was applied, the annoyance score decreased by another 10.7 points to 29.7 points (SD 10.6). Therefore, it can be

considered that the results proposed in this study are also effective from a subjective point of view.

VII. CONCLUSION

In this study, we present a method to actively suppress the driveline noise of a vehicle, which is nonharmonic with engine rotational speed. For active control of the propeller shaft and tire noise, reference signals were generated using the rotation speed of the torque converter and gear ratio in the transmission. The reference signal generated with this approach is used in a control algorithm using an adaptive notch filter. Furthermore, the control strategy is investigated to simultaneously suppress the engine firing order, propeller shaft noise, and tire noise in a passenger car. The proposed control algorithm was implemented in a six-cylinder passenger car to validate the noise suppression performance. Experiments were conducted on noise attenuation of C3 order, the engine firing order, P1, the first order of the propeller shaft, and T2 and T3, which are the second and third harmonics of the tire noise. The experimental results indicate that the C3 order shows an average attenuation of 8.0 dB for entire seat positions. Moreover, the P1, T2, and T3 orders show average attenuations of 5.5 dB, 3.9 dB, and 2.3 dB, respectively. Meanwhile, through subjective evaluation, the annoyance score was found to be 29.7 points after simultaneous control, whereas 46.3 and 82.0 points for EOC and before control, respectively. The results derived from this study were also considered to be indicative of subjective perception.
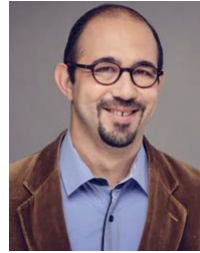
REFERENCES

[1] S. J. Elliott, "A review of active noise and vibration control in road vehicles," Univ. Southampton, Southampton, U.K., ISVR Tech. Memorandum 981, 2008, no. 981.

[2] P. N. Samarasinghe, W. Zhang, and T. D. Abhayapala, "Recent advances in active noise control inside automobile cabins: Toward quieter cars," *IEEE Signal Process. Mag.*, vol. 33, no. 6, pp. 61–73, Nov. 2016.

[3] S.-K. Lee, S. Lee, J. Back, and T. Shin, "A new method for active cancellation of engine order noise in a passenger car," *Appl. Sci.*, vol. 8, no. 8, p. 1394, Aug. 2018.

[4] J. Cheer, "Active sound control in the automotive interior," in *Future Interior Concepts*. Cham, Switzerland: Springer, 2021, pp. 53–69.

[5] Hyundai Motor Company. (2022). *Road-Noise Active Noise Control.* [Online]. Available: https://tech.hyundaimotorgroup.com/article/hyundais-worlds-first-road-noise-active-noise-control-ranc/

[6] Jaguar Land Rover. (2022). *New JAGUAR Noise Cancellation Tech Helps Reduce Driver Fatigue.* [Online]. Available: https://media.jaguarlandrover.com/news/2020/10/new-jaguar-land-rover-noise-cancellation-tech-helps-reduce-driver-fatigue

[7] S. J. Elliott and P. A. Nelson, "Active noise control," *IEEE Signal Process. Mag.*, vol. 10, no. 4, pp. 12–35, Oct. 1993.

[8] N. Zafeiropoulos, J. Zollner, and V. K. Rajan, "State-of-the-art digital road noise cancellation by Harman," in *Automotive Acoustics Conference 2017.* Wiesbaden, Germany: Springer, 2019, doi: 10.1007/978-3-658-20251-4_4.

[9] M. Tahir Akhtar and W. Mitsuhashi, "Improving performance of FxLMS algorithm for active noise control of impulsive noise," *J. Sound Vib.*, vol. 327, nos. 3–5, pp. 647–656, Nov. 2009.

[10] Y. Kajikawa, W. Gan, S. M. Kuo, Y. Kajikawa, and W. Gan, "Recent advances on active noise control?" *APSIPA Trans. Signal Inf. Process.*, vol. 1, no. e3, pp. 1–21, 2015.

[11] N. V. George and G. Panda, "A robust filtered-s LMS algorithm for nonlinear active noise control," *Appl. Acoust.*, vol. 73, no. 8, pp. 836–841, 2012.

[12] N. C. Kurian, K. Patel, and N. V. George, "Robust active noise control: An information theoretic learning approach," *Appl. Acoust.*, vol. 117, pp. 180–184, Feb. 2017.

[13] Y. Xiao, "A new efficient narrowband active noise control system and its performance analysis," *IEEE Trans. Audio, Speech, Language Process.*, vol. 19, no. 7, pp. 1865–1874, Sep. 2011.

[14] M. Bouchard and F. Albu, "The Gauss–Seidel fast affine projection algorithm for multichannel active noise control and sound reproduction systems," *Int. J. Adapt. Control Signal Process.*, vol. 19, nos. 2–3, pp. 107–123, Mar. 2005, doi: 10.1002/acs.846.

[15] F. Albu and C. Paleologu, "New multichannel modified filtered-x algorithms for active noise control using the dichotomous coordinate descent method," in *Proc. Eur. Conf. Noise Control*, no. 1, 2008, pp. 5723–5727, doi: 10.1121/1.2935769.

[16] Analog Devices. (2022). *Active Noise Cancellation.* [Online]. Available: https://www.analog.com/en/applications/markets/automotive-pavilion-home/cabin-electronics-and-infotainment/active-noise-cancellation.html/

[17] Texas Instruments. (2022). *Jacinto^{TM} 7 Processors in Automotive Applications.* [Online]. Available: https://training.ti.com/jacinto7

[18] S. M. Kuo and D. R. Morgan, *Active Noise Control Systems*, vol. 4. New York, NY, USA: Wiley, 1996.

[19] Y. Hinamoto and H. Sakai, "Analysis of the filtered-X LMS algorithm and a related new algorithm for active control of multitonal noise," *IEEE Trans. Audio, Speech Language Process.*, vol. 14, no. 1, pp. 123–130, Jan. 2006, doi: 10.1109/TSA.2005.854089.

[20] R. Schirmacher, "Active noise control and active sound design-enabling factors for new powertrain technologies," SAE Tech. Papers 2010-01-1408, 2010.

[21] R. Schirmacher, R. Kunkel, and M. Burghardt, "Active noise control for the 4.0 TFSI with cylinder on demand technology in Audi's S-series," SAE Tech. Papers 2010-01-1408, 2012.

[22] J. Krüger, F. Castor, and R. Jebasinski, "Active exhaust silencers—Current perspectives and challenges," SAE Tech. Papers 2007-01-2204, 2007.

[23] M. Moetakef, A. Bresky, M. Zilberman, T. Pham, R. Egenolf, and B. Bonhard, "Reducing high frequency driveshaft radiated noise by polymer liners," SAE Tech. Papers 2005-01-3554, 2005.

[24] M. Bozca, "Torsional vibration model based optimization of gearbox geometric design parameters to reduce rattle noise in an automotive transmission," *Mech. Mach. Theory*, vol. 45, no. 11, pp. 1583–1598, Nov. 2010, doi: 10.1016/j.mechmachtheory.2010.06.014.

[25] N. Inavolu, S. N. Kumar, K. Kamani, and M. J. Rao, "Driveline noise source identification and reduction in commercial vehicles," SAE Tech. Papers 2018-01-1474, 2018.

[26] G. Steyer, M. Voight, and Z. Sun, "Balancing competing design imperatives to achieve overall driveline NVH performance objectives," SAE Tech. Papers 2005-01-2308, 2005.

[27] T. Wolff, "Aspects of driveline integration for optimized vehicle NVH characteristics," SAE Tech. Papers 2007-01-2246, 2007.

[28] Y.-D. Kim, "Driveline vibration reduction of FR(front engine rear wheel drive) vehicle at rapid acceleration," *Trans. Korean Soc. Noise Vib. Eng.*, vol. 24, no. 8, pp. 592–599, Aug. 2014.

[29] M. S. Qatu, R. King, R. Wheeler, and O. Shubailat, "Vehicle design for robust driveline NVH due to imbalance and runout using a Monte Carlo process," *SAE Int. J. Passenger Cars, Mech. Syst.*, vol. 4, no. 2, pp. 1033–1038, May 2011, doi: 10.4271/2011-01-1546.

[30] J. Yang and T. C. Lim, "Influence of propeller shaft bending vibration on drivetrain gear dynamics," *Int. J. Automot. Technol.*, vol. 16, no. 1, pp. 57–65, Feb. 2015.

[31] Z. Sun, D. Schankin, W. Braun, and J. Ley, "Attenuation of driveline vibrations through tuning of propeller shaft liners," SAE Tech. Papers 2011-01-1547, 2011.

[32] F. M. F. Novo, M. M. De Souza, J. Savoy, and M. A. D. C. Silva, "Analysis of the vibration modes of an automotive propeller shaft using FEM and analytical models," SAE Tech. Papers 2012-36-0224, 2012.

[33] T. Inoue, A. Takahashi, H. Sano, M. Onishi, and Y. Nakamura, "NV countermeasure technology for a cylinder-on-demand engine-development of active booming noise control system applying adaptive notch filter," SAE Tech. Papers 2004-01-0411, 2004.

[34] S. Elliott, *Signal Processing for Active Control*. Amsterdam, The Netherlands: Elsevier, 2000.

[35] S. Becker, C. Beyer, and R. McAfee, "1st order boom noise relationship to driveline imbalance," SAE Tech. Papers 2005-01-2299, 2005.

[36] V. A. J. Britto, S. Karmakar, M. Muthuveeraswamy, and B. Natarajasundaram, "High speed booming noise reduction in passenger car by application of cost optimized NVH solution," SAE Tech. Papers 2016-28-0039, 2016.

[37] M. R. Vikram, M. Gehringer, and R. Patil, "Dual degree of freedom vibration damper (DDVD) for driveline noise and vibration issue resolution," SAE Tech. Papers 2015-01-2177, 2015.

[38] B. Rohrmann, "Verbal qualifiers for rating scales: Sociolinguistic considerations and psychometric data," Univ. Melbourne, Melbourne, VIC, Australia, Project Rep., 2007, pp. 1–28. [Online]. Available: http://www.rohrmannresearch.net/pdfs/rohrmann-vqs-report.pdf

M. ERCAN ALTINSOY received the degree in mechanical engineering from the Technical University of Istanbul, Istanbul, Turkey, and the Ph.D. degree in electrical engineering from Ruhr-University Bochum, Bochum, Germany, in 2005.

After his receiving the Ph.D. degree, he worked with HEAD Acoustics as a Consulting Engineer. Since 2006, he has been with Technische Universität Dresden, Dresden, Germany. He is currently a Professor of acoustic and haptic engineering with Technische Universität Dresden. His main research interests include perception-based engineering, vibroacoustics, vehicle acoustics, electroacoustics, haptic interfaces, haptic perception, whole-body vibrations, product sound, and vibration design.

Dr. Altinsoy was a member of the International Graduate School for Neuroscience with Ruhr-University Bochum. He is a Lothar-Cremer medalist of the Acoustical Society of Germany, DEGA. In 2018, he was awarded as a Visiting Professorship from Tohoku University, Japan. He is the Chairman of the Vehicle NVH Expert Committee of DEGA and one of the core team members of the cluster of excellence Centre for Tactile Internet With Human-in-the-Loop.

• • •

SEONGHYEON KIM received the B.S. and M.S. degrees in mechanical engineering from Hanyang University, South Korea, in 2004 and 2006, respectively. He is currently pursuing the Ph.D. degree in electronic and computer engineering with Technische Universität Dresden, Dresden, Germany.

From 2006 to 2011, he was a Senior Research Engineer with the Chief Technology Officer Division, LG Electronics, Seoul, South Korea. Since 2011, he has been a Senior Research Engineer with the Institute of Advanced Technology Development, Hyundai Motor Group, Gyeonggi-do, South Korea. His research interests include active sound control, active sound design, sound quality, multisensory perception and reproduction, and vehicle NVH.